HIGH FREQUENCY EFFECTS AND PERFORMANCE OF A 600 GHz - 635 GHz SIS RECEIVER USING Nb/AlOx/Nb JUNCTIONS

M. Salez, P. Febvre*, W. R. McGrath, B. Bumble, H. G. LeDuc

Jet Propulsion Laboratory, 4800 Oak Grove Drive, 91109 Pasadena
DEMIRM -Observatoire de Paris-Meudon, 5 place Jules Janssen, 92195 Meudon, France

ABSTRACT

A 600 GHz - 635 GHz waveguide SIS heterodyne receiver was built and used for astronomical observations at the Caltech Submillimeter Observatory (CSO) in Hawaii. The mixer employs a 0.25-μm^2 Nb/AlOx/Nb junction integrated with a Nb/SiO/Nb microstrip tuning circuit. The double sideband receiver noise temperature is 245 K - 310 K over the tunable bandwidth. At frequencies approaching the gap frequency of niobium (700 GHz), the optimization of the receiver is limited by the overlap of second-order and first-order photon steps of opposite signs. A noise increase of 10% - 40% is measured when the junction is biased in the region where the photon steps overlap, in agreement with the calculations using Tucker's theory. The bias range yielding the best performance is a small portion of the photon step in the vicinity of the second Shapiro step, which makes the cancellation of the AC Josephson effect with an external magnetic field critical.

1. INTRODUCTION

The importance for radioastronomy of molecular rotational lines at submillimeter wavelengths has led to the development of low-noise heterodyne receivers. The most sensitive spectrometers at millimeter and submillimeter wavelengths make use of quasiparticle SIS (Superconductor-Insulator-Superconductor) mixers [1 - 9], for which the quantum mixer theory predicts both high RF-to-IF conversion efficiency and quantum-limited noise [10]. SIS mixers

are expected to work well at frequencies up to the gap frequency of the superconductor used, and up to twice this frequency with a somewhat degraded performance [11-13]. While some preliminary measurements have been done on low energy gap superconductors, like aluminum [14], at millimeter wavelengths, few experimental studies have been performed at submillimeter wavelengths near the energy gap.

Almost all SIS receivers presently used on radiotelescopes use niobium junctions for their ruggedness and high quality *I-V* characteristics. Recently, a few niobium-based receivers have been operated on telescopes [1 - 5] and aboard airplanes [6, 7] at frequencies approaching 700 GHz, the gap frequency of niobium. Furthermore, the use of SIS mixers at still higher frequencies has been demonstrated in the laboratory [8]. The SIS receiver described here was designed to operate at frequencies around 625.9 GHz to allow for the detection of hydrochlorine in the interstellar medium and planetary atmospheres. This frequency range also provides a unique opportunity to investigate several consequences of operating an SIS receiver near the gap frequency. In particular, we find an increase of the receiver noise at bias voltages where the photon steps overlap, as predicted by theory.

2. RECEIVER DESCRIPTION

An extensive discussion of the receiver design has been given elsewhere [15]. The mixer uses a single $Nb/AlO_x/Nb$ junction of area 0.5 μm $\times$ 0.5 μm. The junctions are fabricated from a DC-sputtered trilayer using electron-beam lithography, with a self-aligned insulator lift-off technique which has been described previously [16]. The junction critical current density is 11 kA/cm^2 and its normal resistance at 4.2 K is $R_N \approx 73$ Ω. The capacitance per unit area is estimated to be 100 $fF/\mu m^2$, and hence $C \approx 25$ fF. The value of $\omega R_N C$ is ~ 6.8 at 600 GHz, and thus the geometric capacitance significantly shunts the RF signal from the quasiparticle tunneling conductance.

In order to optimize the RF impedance match, a superconductive microstrip circuit is integrated with the junction which tunes out the capacitance C by providing a distributed inductance ~ $1/\omega^2 C$ in parallel. Figure 1 shows the particular circuit which has yielded the best receiver noise results so far. It consists of a quarter-wavelength microstrip stub which provides a wide-band RF

short, used in combination with a 25-μm long, 5-μm wide section of transmission line which transforms this RF short into the appropriate inductance. This circuit design and its calculated performance are discussed elsewhere [15,17].

The fused-quartz substrate with the SIS junction and the integrated superconductive circuit is placed in a waveguide mount along the E-field direction across a 170 μm rectangular waveguide. The radiation is coupled into this waveguide via a dual-mode conical feedhorn [18].

A backshort and an E-plane tuner are used to match the junction RF complex impedance. Both tuners are of the contacting type. A symmetrical RF choke filter prevents the submillimeter-wave radiation from leaking out of the waveguide through the bias/IF leads.

The local oscillator (LO) consists of a 100 GHz - 106 GHz Gunn source followed by x2 x3 whisker-contacted Schottky varactor multipliers [19]. A harmonic mixer with an internal -10 dB coupler is inserted between the Gunn oscillator and the multipliers to provide a reference signal for a phase-lock system.

The low-noise IF amplifier is a 3-stage HEMT (High Electron Mobility Transistor) amplifier from Berkshire Technologies [20], cooled to 13 K. The amplifier gain and noise temperature, specified at 77 K, are 33 dB and 2-3 K over nearly 800 GHz of bandwidth centered at 1.4 GHz.
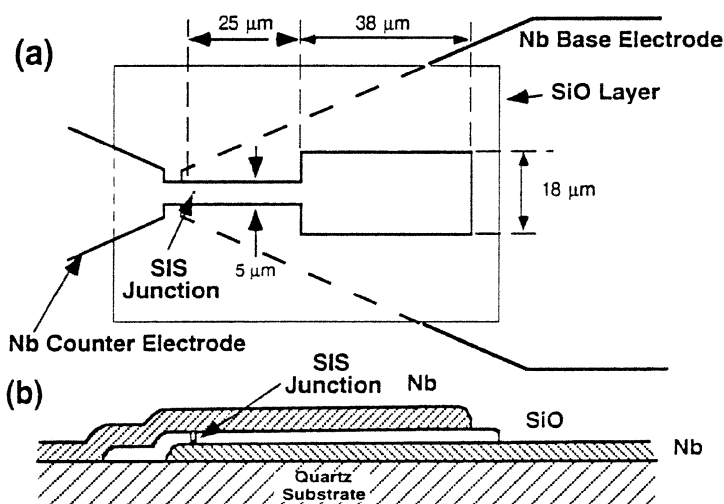

Fig. 1. Top (a) and cross-section (b) views of the microstrip Nb/SiO/Nb tuning circuit integrated with the junction (not to scale).

To average out the Josephson currents which are a source of noise in a quasiparticle mixer, a coil of superconducting NbTi wire produces a magnetic field of up to 1000 Gauss aligned with the plane of the junction. This is sufficient to apply at least three magnetic flux quanta within the junction since the magnetic field corresponding to one flux quantum (2×10^{-15} Wb) is about 300 Gauss.

The mixer and the optics are mounted on a 4-liter liquid helium tank, which cools the components to about 4.5 K by thermal conduction. In addition, a closed-cycle helium refrigerator cools two concentric jackets surrounding the helium tank down to 13 K and 80 K. Under typical operating conditions, the measured receiver hold time is about 5 days.

3. RECEIVER PERFORMANCE

In Fig. 2, the double-sideband (DSB) receiver noise power per unit bandwidth (expressed in temperature units using the Rayleigh-Jeans formula $P/B = kT$) is plotted versus LO frequency. The frequency range of the receiver is presently set by the local oscillator. For each point, the backshort and E-plane tuner positions, the LO power, the bias voltage and the magnetic field have been optimized. The best noise temperature is 245 K ± 15 K at 610 GHz. The frequency response is relatively flat and the noise rises to 330 K ± 19 K at 635 GHz. The variations of T_R across the IF bandwidth have also been measured, with a tunable 40-MHz bandpass filter. The receiver noise varies smoothly within the IF bandwidth of ~ 600 MHz. T_R was derived using the 'Y-factor' method, i.e., from the relation

$$T_R = (T_h - Y T_c) / (Y - 1) \qquad (3)$$

where Y is the ratio P_h/P_c of the IF output powers measured in response to a hot (T_h = 295 K) and a cold (T_c = 82 K) *Eccosorb* load placed at the receiver RF input. The IF bandwidth for the noise measurements was 500 MHz. The response of the receiver to the hot and cold loads can be seen in Fig. 3.
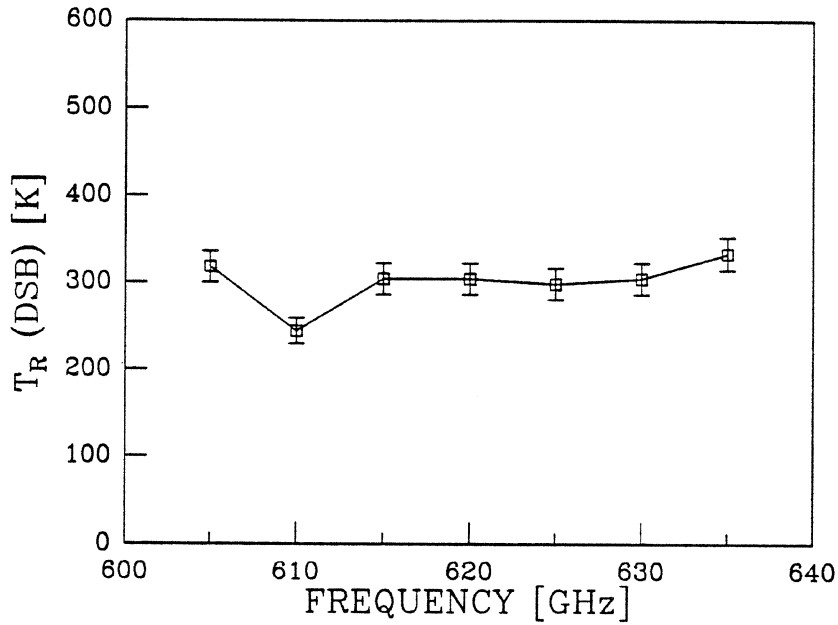
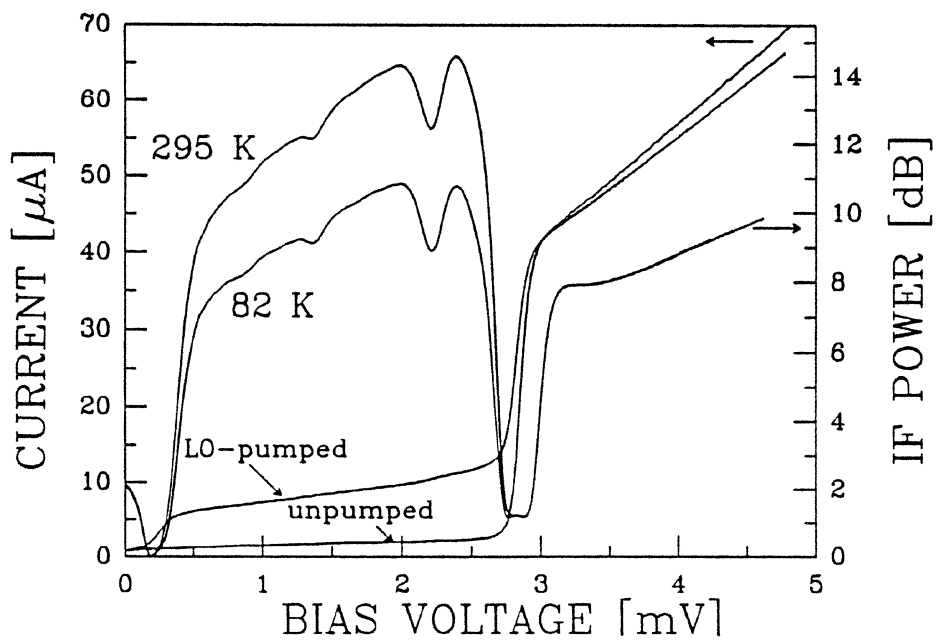Fig. 2.   Double-sideband receiver noise temperature versus LO frequency.

Fig. 3. Typical IF output power versus bias voltage, for a hot (295 K) and a cold (82 K) load presented to the receiver input. Superimposed are the unpumped and the corresponding LO-pumped *I-V* characteristics.

4. OVERLAP OF PHOTON STEPS

4.1. Experimental observations

Figure 3 shows the typical IF power response of the receiver for the hot (295 K) and cold (82 K) loads, as a function of the bias voltage. The LO-pumped and unpumped *I-V* characteristics are also shown. The magnetic field applied in the plane of the junction has completely zeroed the amplitude of the Shapiro steps and the corresponding flux is one flux quantum $\Phi_0 = h/2e$.

A minimum at 2.2 mV followed by a peak at 2.4 mV, is seen in the IF output power. This feature was seen in all IF power curves for all LO frequencies, although its exact voltage location in the upper part of the photon step varies directly with frequency. The peak is always close to where one expects the second Shapiro step, but its amplitude remains unchanged by a magnetic field applied to the junction. Furthermore, the 2nd Shapiro step could be seen as an *independent*, much narrower and noisier component, the amplitude of which could be strongly affected by the applied magnetic field.

The feature was seen for all LO powers above a certain level, and is enhanced with large LO powers. In Fig. 4, which shows experimental data for a large LO pumping level, one can easily detect an inflection point in the pumped current-voltage characteristic at the voltage where the narrow minimum in the IF output power (now sharper and deeper) occurs. The voltage at which inflection point and IF power-drop occur turns out to be identical.

4.2. Predicted photon step overlap

The inflection point in the pumped *I-V* curve and the sharp minimum in the IF power curve both result from the overlap of the $n = 1$ photon step of the positive voltage region with the $n = 2$ photon step from the negative voltage region (see Fig. 5). The latter decreases the pumped current in the region of overlap, hence causing an inflection point in the former. Part of the drop in the IF output power is due to a poorer coupling at the inflection point, where the IF impedance is smaller than on the rest of the photon step. In addition, the mixer conversion loss is proportional to the IF conductance, and hence exhibits a change at any voltage where the conductance varies sharply. This "photon-step-overlap" interpretation is a convenient way for describing the shape of an RF-
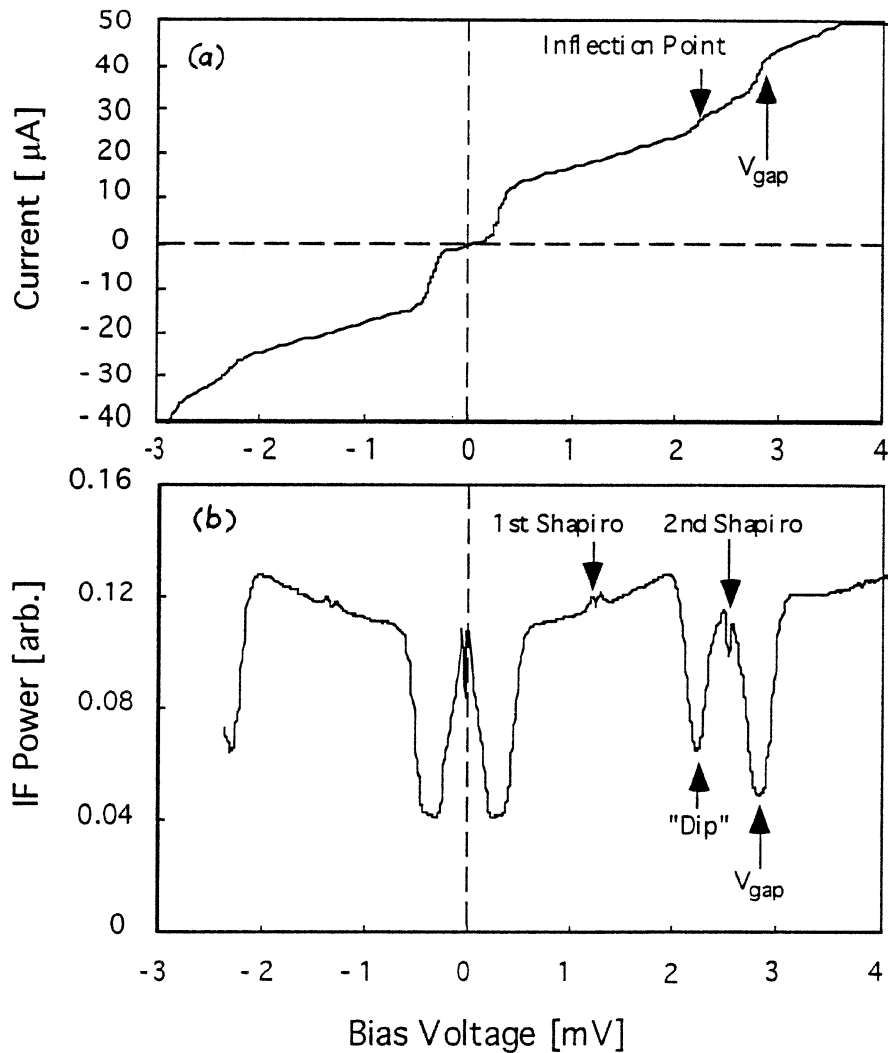
Fig. 4. (a) LO-pumped I-V curve and (b) receiver IF output power versus bias voltage with the hot load at the receiver input for $\Phi = \Phi_0$ and a large LO power, at f = 635 GHz.

pumped SIS I-V curve, which is antisymmetric about the origin.

The fact that high LO powers enhance the inflection point in the pumped I-V curves supports this interpretation. Furthermore, the inflection point voltage is directly correlated with the voltage expected for the overlap

$$V^{\,overlap} = 2\ h\omega/e - V_g \qquad (4)$$

as the experimental points plotted in Fig. 6 demonstrate. In Eq. (4), $V^{\,overlap}$ is defined as shown in Fig. 5, h is Planck's constant, ω is the angular frequency, and V_g is the junction gap voltage. For comparison, the voltage corresponding to the

$n = 2$ Shapiro step has also been plotted and conforms to the Josephson voltage-frequency relation

$$V^{shapiro} = 2\ (h\omega/2e) \tag{5}$$

For sufficiently high LO powers, a minimum in the coupled IF power could also be observed *above* the gap, involving the $n = 3$ negative photon step, at

$$V^{overlap'} = 3\ h\omega/e - V_g \tag{6}$$

This effect is predicted by the Tucker theory and has been observed in Al-based junctions at 73 GHz [14]. It has not been mentioned in the literature so far at higher frequencies, possibly because its appearance in niobium mixers is limited to frequencies between 470 GHz and 690 GHz (see section 4.4) and only a few SIS receivers have been reported in this range. Also, the effect of the overlap is LO-power dependent, and not all SIS receivers require the same amount of LO power when optimized.
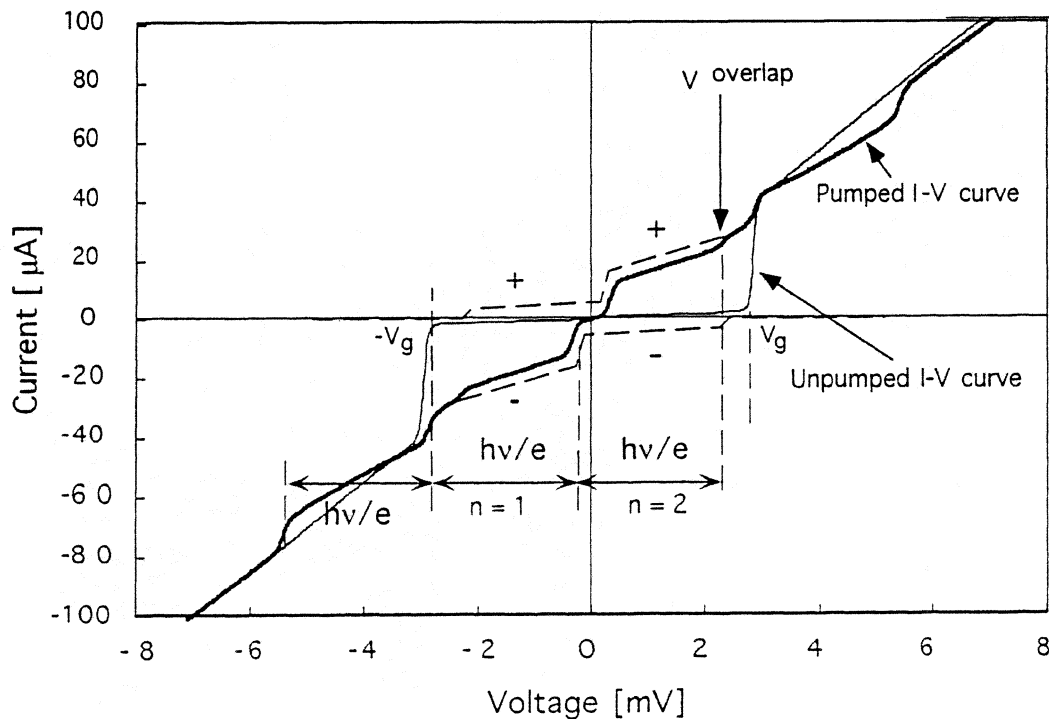

Fig. 5. Schematic reconstruction of an experimental pumped *I-V* curve displaying an inflection point (heavy line) using the photon step overlap argument. The dashed curves show the photon steps of width *hv/e* from the positive and negative voltage regions "before" their effects are added.
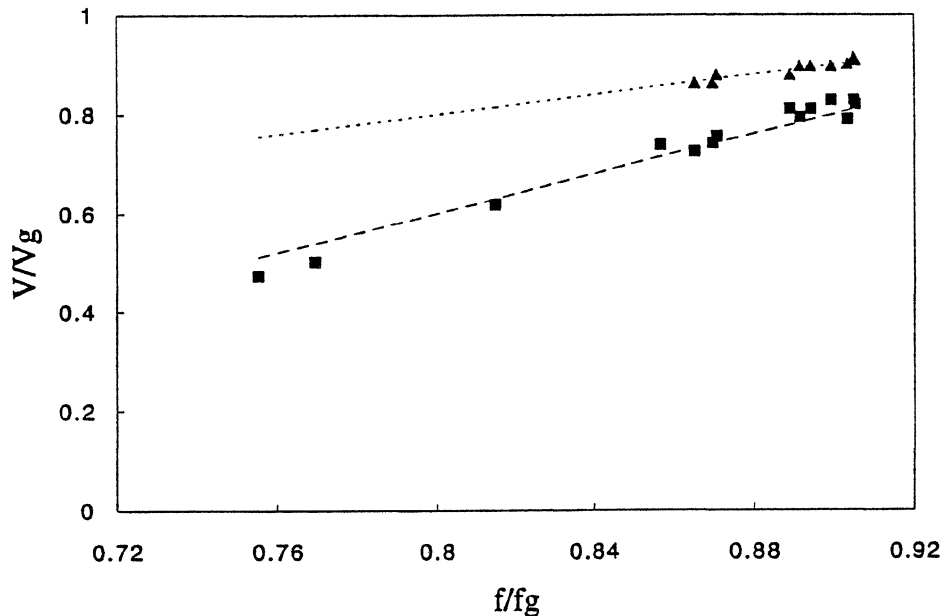
Fig. 6. Measured voltages for the inflection point (squares), normalized to the gap voltage $h f_g/e$, as a function of the normalized LO frequency f/f_g. The dashed line represents the predicted voltages for the photon step overlap. For comparison, the 2nd Shapiro steps (triangles) are also shown and compared to the prediction (dotted line).

We have experimentally and theoretically investigated how this overlap affects the performance of a submillimeter-wave receiver. We have systematically measured the increase in receiver noise in the overlap region for several frequencies between 600 GHz and 635 GHz and for various LO power levels. We find that when biased at voltages where the photon steps overlap, the receiver exhibits a noise typically higher by 10%-40%. Although not prohibitive for the use of an SIS receiver, this is a significant reduction in performance.

4.3. Theoretical fits

We have performed theoretical calculations using the Tucker theory to analyze the inflection point caused in the pumped I-V curves by the photon step overlap, and to investigate the predicted effect on the mixer noise temperature and gain. The numerical program fits pumped I-V curves and thus provides the LO power applied to the SIS junction and the embedding impedance of the mixer [12]. Calculated pumped I-V curves can then be generated for any LO pumping level, and the corresponding available mixer gain and mixer temperature can be calculated as a function of the bias voltage. In addition, the measured noise and gain of the IF system have been included in order to predict the increase in *receiver* noise and the receiver output IF power for the hot RF load.

Figure 7(a) shows a calculated pumped I-V curve fitting experimental data at 631.14 GHz. The corresponding LO power is $P_{LO} = 125.7$ nW. The embedding impedance $Z = 17.8 - j$ 42.7 Ω used for the calculation has been derived first, by fitting the experimental pumped I-V characteristic. The experimental values of the receiver noise temperature and of the receiver IF output power for the RF hot load as a function of the bias voltage are shown in Fig. 7(b). The calculated IF output power for the hot load and the DSB receiver noise temperature are shown in Fig. 7(c) along with the available and coupled mixer gains.

The dip observed in the IF power output in Fig. 7(b) at the inflection point proves not only to be an effect of IF mismatch, but also to correspond to a sharp decrease of the *available* mixer gain at V ^{overlap}, which is proportional to the mixer IF resistance. Qualitatively and quantitatively, the agreement between the calculated and measured receiver noise *variations* is good, despite the uncertainties intrinsic to this type of calculation. A noise increase of about 100% is predicted as one biases the mixer from $V >$ V ^{overlap} to $V <$ V ^{overlap}. In the data, a receiver noise variation of nearly 40% is observed. This level of LO pump is close to the level required to optimize the receiver performance.

4.4. Consequences for SIS receiver operation

The photon step overlap described above has practical consequences for submillimeter wave receivers. Near the superconductor energy gap frequency, the voltage range where the best mixer performance can be obtained is restricted to only a small fraction of the photon step. The frequency for which an overlap starts 'eating away' the bias region on the first photon step can be simply expressed by:

$$ f = \left(\frac{2}{n+1} \right) \cdot f_g \tag{7} $$

where n is the order of the photon step of opposite sign to be considered. From this equation, one sees that the $n = 3$ photon step plays a role at $f > f_g/2$, that is $f > 350$ GHz in the case of a niobium mixer. However, for the typical levels of LO power involved in receiver operation, the effect on the noise of this 3rd step is negligible.
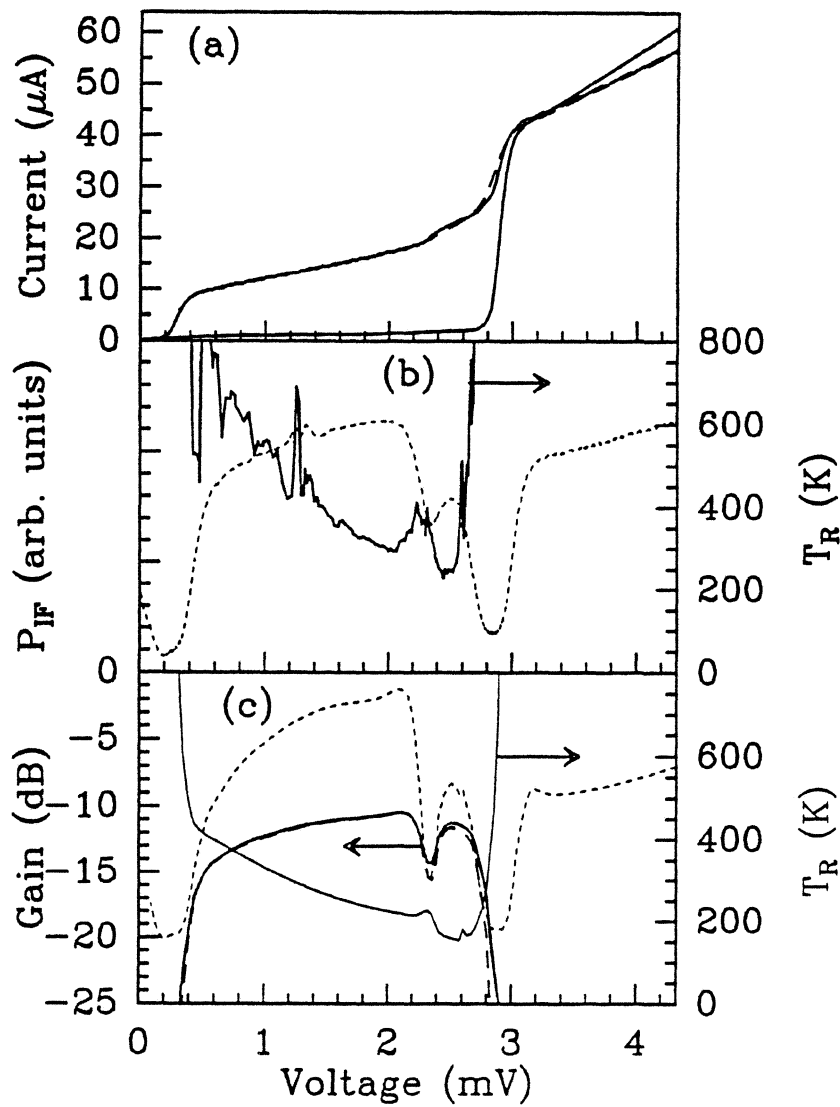
Fig. 7. (a) Unpumped I-V curve and measured (dashed) and calculated (solid) pumped I-V curves at 631 GHz for $P_{LO} = 125$ nW; (b) measured double-sidebandT_{rec} and P_{IF} (295 K) versus bias voltage; (c) calculated T_{rec} and P_{IF} (295 K) versus bias voltage along with the available (solid) and coupled (dashed) mixer gains G_{mix}^a and G_{mix}^c.

The case $n = 2$ occurs at frequencies higher than $2/3 f_g$, or 466 GHz. At 547 GHz, the overlap is observed [9] but is of little importance for receiver operation as a large part of the photon step can still be used to bias the junction with an optimum noise. However, this region shrinks as the frequency increases and ends up corresponding to a very narrow peak in the IF power curves. At 600 - 635 GHz, the change with frequency is big and this effect has a strong impact on biasing the junction to obtain the lowest noise possible. At frequencies around 660 - 690 GHz, this region is already vanishingly small, allowing no practical bias at $V > V^{overlap}$, and the effect discussed here would be unnoticed [4,5].

At frequencies above 700 GHz ($n = 1$), niobium-based SIS mixers can perform reasonably well [8] but the response degrades because the $n = 1$ and $n = 2$ photon steps completely overlap. In addition, the mixer can then only be operated at $V > h\omega/e - V_g$ because of the overlapping $n = 1$ photon step from the negative region. Nevertheless, this problem could be circumvented if the amount of LO power required to operate the mixer was lower, which is in theory possible with different mixer RF source impedances [22]. The final limit to the use of niobium SIS mixers is at 1400 GHz ($n = 0$), i.e. *twice* the gap frequency of niobium, when the $n = 1$ photon step from either side covers the entire $(-V_g , V_g)$ bias range.

At 600 - 635 GHz, the photon step overlap has another consequence on the biasing conditions. Coincidentally, the small portion of the photon step where one should bias to yield the best performance is *in the vicinity of the second Shapiro step*. It is obvious from Fig. 6 that as the frequency increases, the locations of the Shapiro step and of the discussed overlap *converge*, hence making biasing more restricted. This is not yet a problem at 547 GHz [9], but becomes of concern at 600 GHz and above. Therefore, the perfect cancellation with an external field of the AC Josephson effect is critical to avoid instabilities and additional noise.

The suppression of the Shapiro steps by the application of a suitable magnetic field is always possible in theory. However in practice, noise spikes often remain in the IF power at the Shapiro voltages although the *I-V* characteristics looks completely smoothed. It is not clear how well a flux quantum which averages out completely the DC Josephson current does in averaging out the AC counterpart which can mix down to the IF frequency.

The averaging process may be more efficient for a larger number of applied flux quanta, but then, the intense magnetic field may slightly *reduce* the gap of the junction, as shown in Fig. 8 for $\Phi \sim 3\ \Phi_0$. Not only does the gap voltage decrease for a large magnetic field, but as a result $V^{overlap}$ given by eq. (4) also becomes higher. These two effects add up to further reduce the bias region of lowest noise. In the example of Fig. 8, one has $V_g^{reduced} \sim V^{overlap}$, meaning that the voltage region where there is no overlap has disappeared.
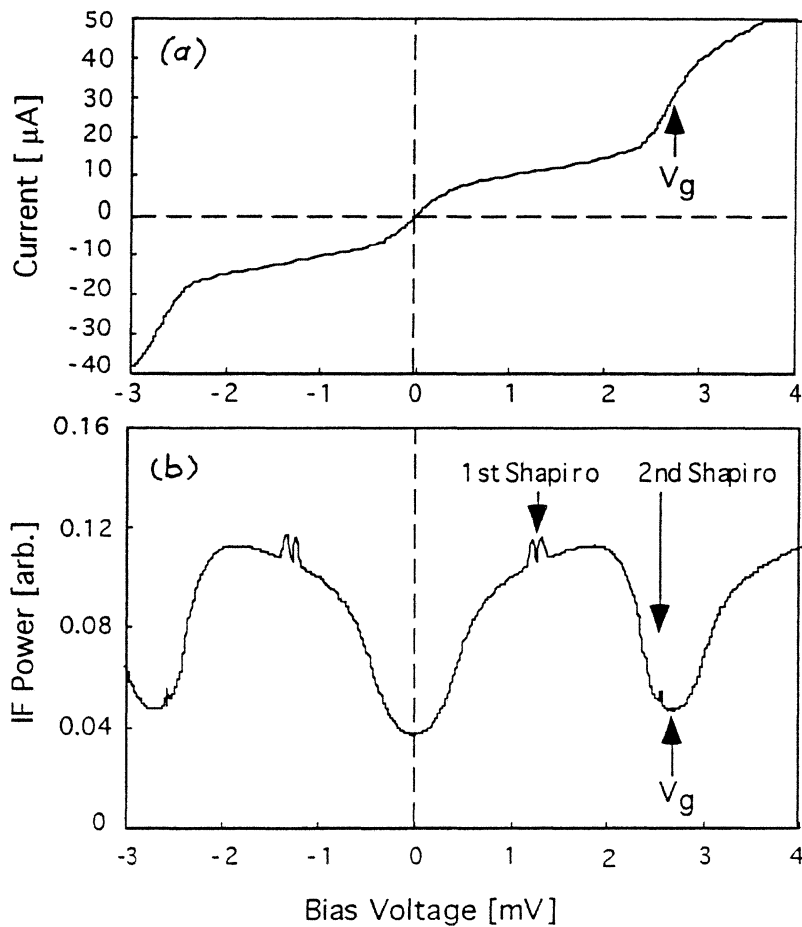
Fig. 8. Measured LO-pumped *I-V* characteristics (a) and P_{IF} (295 K) (b) for an applied magnetic flux of $\Phi = 3\ \Phi_0$ at $f = 635$ GHz. The second Shapiro step and the overlap-induced inflection point are now located at the magnetically-reduced gap voltage.

V. OBSERVATIONS AT THE CSO

The receiver was installed at the Cassegrain focus of the 10.5-m CSO telescope, on Mauna Kea in Hawaii, in November 1993. The weather was exceptionally good, and for a DSB receiver noise temperature on site of 250 K - 350 K, the system noise temperature, which is dominated by the atmospheric attenuation, ranged from 2000 K to 8000 K DSB, varying with frequency, day, and zenith angle. The receiver was tuned at each frequency for the optimum Y-factor and biased on the best performance region discussed earlier. In terms of trapped flux and coupled LO power, the receiver was very stable throughout the night, as determined from frequent sweeps of the *I-V* curve for check-up. The externally applied flux was less than two flux quanta to avoid a gap reduction, and the $n = 2$ Shapiro step could always be completely quenched in the IF output power curve.

Both $H^{35}Cl$ and $H^{37}Cl$ isotopes were detected in emission in several molecular clouds, along with other molecules in the 600 GHz - 636 GHz range. Figure 9 shows the spectrum of a particular region of the molecular cloud OMC-1 in Orion, with the expected hyperfine structure of the $H^{35}Cl$ (J=1-0) transition at 625.92 GHz.
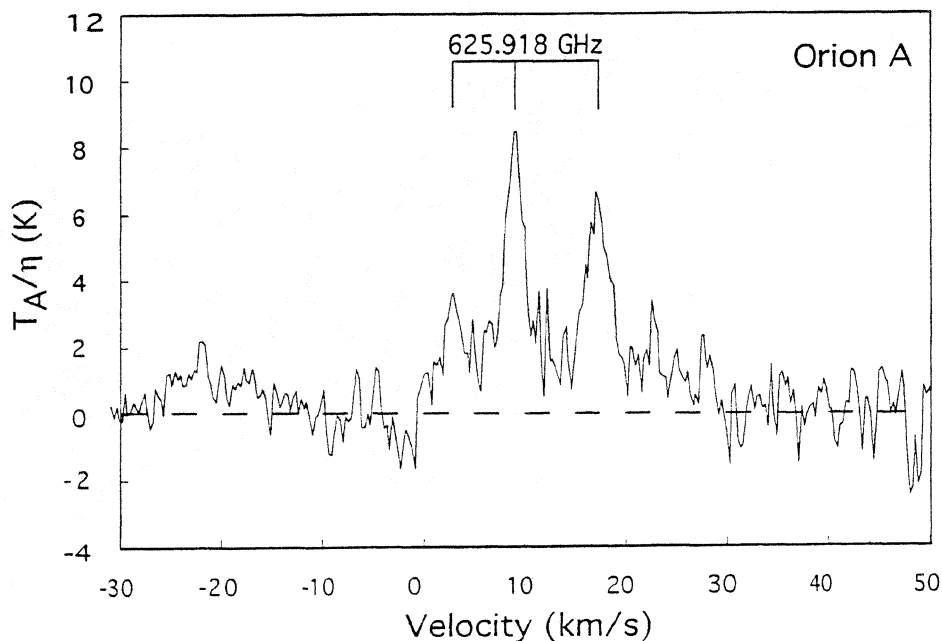

Fig. 9. Spectrum of the $H^{35}Cl$ (J=1-0) line at 625.918 GHz, taken in a region of Orion A with an integration time of 30 minutes (T_{sys} = 6550 K). All three hyperfine lines are seen.

7. CONCLUSION

We have discussed the performance of a waveguide SIS heterodyne receiver using a submicron Nb/AlOx/Nb junction and a niobium-based integrated tuning circuit, in the frequency range 600 GHz - 635 GHz, i.e. as high as 90% of the niobium gap frequency of 700 GHz. The lowest noise temperature of the receiver is 245 K DSB, and is close to 300 K DSB elsewhere in the LO frequency range. At these frequencies, the performance of the receiver is somewhat limited by the overlap of the second-order and first-order photon steps of opposite signs. In the bias region where the steps overlap we have measured a receiver noise increase of 10% - 50%, depending on the amount of LO power. This noise increase is qualitatively and quantitatively consistent with theoretical calculations using the Tucker theory. As the frequency of operation is increased, the fraction of the photon step where one expects the best performance is reduced to a small region, undesirable because of its proximity with the second Shapiro step, and shrinking to zero as the frequency approaches 700 GHz. Furthermore, an intense magnetic field applied to suppress the Josephson currents may further reduce the availability of this region. At frequencies higher than 700 GHz, this photon step overlap modifies the operating conditions of niobium-based SIS receivers and particular attention must be paid to optimize the LO level and source impedance. This receiver was successfully operated and used for astronomical observations at the CSO telescope, in Hawaii.

8. ACKNOWLEDGEMENTS

IX. REFERENCES

[1]   A. Karpov, M. Carter, B. Lazareff, M. Voss, D. Billon-Pierron, K.H. Gundlach, *Proc. 4th Internat. Symp. on Space Terahertz Technology*, p. 11, UCLA, CA (1993).

[2]   C.K. Walker, J.W. Kooi, M. Chan, H.G. LeDuc, P.L. Schaffer, J.E. Carlstrom and T.G. Phillips, *Proc. 3rd Internat. Symp. on Space Terahertz Technology*, p. 266, University of Michigan, MI (1992).

[3]   B.N. Ellison, S.M.X. Claude, A. Jones, D.N. Matheson, L.T. Little and S.R. Davies, *Proc. 18th Internat. Conf. on Infrared and Millimeter Waves*, p. 106, Colchester, U.K. (1993).

[4]   J. Kooi, these proceedings.

[5]   K. Schuster, A.I. Harris, K.H. Gundlach, Int. J. of Infrared and Millimeter Waves **14**, (10) pp. 1867-1887 (1993).

[6]   J. Zmuidzinas, HG. LeDuc, J.A. Stern, S.R. Cypher, *Proc. 4th Internat. Symp. on Space Terahertz Technology*, p. 72, UCLA, CA (1993).

[7]   J. Mees, these proceedings.

[8]   G. DeLange, C.E. Honingh, M.M.T.M. Dierichs, H.H.A. Schaeffer, H. Kuipers, *Proc. 4th Internat. Symp. on Space Terahertz Technology*, p. 41, UCLA, CA (1993).

[9]   P. Febvre, W.R. McGrath, P. Batelaan, H.G. LeDuc, B. Bumble, M.A. Frerking and J. Hernichel, *Digest of IEEE MTT-S Int. Microwave Symposium*, p. 771, Atlanta, GA (1993) ; *Proc. 18th Internat. Conf. on Infrared and Millimeter Waves*, p. 263, Colchester, U.K. (1993).

[10]   J.R. Tucker, Appl. Phys. Lett. **36**, 477 (1980).

[11]   M.J. Feldman, Internat. J. of Infrared and Millimeter Waves **8**, 1287 (1987).

[12]   W.C. Danchi and E.C. Sutton, J. Appl. Phys. **60**, 3967 (1986).

[13]   Tek-Ming Shen, IEEE J. of Quant. Electronics **QE-17**, 1151   (1981).

[14]   D. Winkler and T. Claeson, J. Appl. Phys. **62**, 4482 (1987).

[15]   M. Salez, P. Febvre, W.R. McGrath, B. Bumble, H.G. LeDuc, Internat. J. of Infrared and Millimeter Waves **15**, (6) 349 (1994).

[16]   H.G. LeDuc, B. Bumble, S.R. Cypher, A.J. Judas and J.A. Stern, *Proc. 3rd Internat. Symp. on Space Terahertz Technology*, p. 408, University of Michigan, MI (1992).

[17]   P. Febvre, W.R. McGrath, P. Batelaan, H.G. LeDuc, B. Bumble, to appear in Internat. J. of Infrared and Millimeter Waves **15**, (6) (June 1994).

[18]   H.M. Pickett, J.C. Hardy, J.C. and J. Farhoomand, IEEE Trans. Microwave Theory and Techn. **MTT-32**, 936 (1984).

[19]   Radiometer Physics, Bergerwisen Straß 15, 53340 Meckenheim, Germany.

[20]   Berkshire Technologies Inc., 5427 Telegraph Ave, Oakland, CA.

[21]   A. Skalare, Int. J. Infrared and Millimeter Waves 10 (11) (1989).

[22]   P. Febvre, these proceedings.